[Fp*Fc][PF$_6$]: A Remarkable Non-symmetric Dinuclear Cation in a Very Stable Mixed-Valent State

Gilles Argouarch,[†] *Guillaume Grelaud,*[†,‡] *Thierry Roisnel,*[§] *Mark G. Humphrey,*[*,‡] *and Frédéric Paul*[*,†]

[†] Institut des Sciences Chimiques de Rennes, CORINT, UMR CNRS 6226, Université de Rennes 1, Campus de Beaulieu, 35042 Rennes Cedex, France

[‡] Research School of Chemistry, Australian National University, Canberra, ACT 2601, Australia

[§] Institut des Sciences Chimiques de Rennes, Centre de Diffractométrie X, UMR CNRS 6226, Université de Rennes 1, Campus de Beaulieu, 35042 Rennes Cedex, France

E-mail: frederic.paul@univ-rennes1.fr

Tel: (+33) 02 23 23 59 62

E-mail: gilles.argouarch@univ-rennes1.fr

Tel: (+33) 02 23 23 59 61

E-mail: mark.humphrey@anu.edu.au

Tel: (+61) 2 61 25 29 27

Dedicated to Professor John A. Gladysz, on the occasion of his 65th birthday, for his scientific contribution to the chemistry of mixed-valence complexes and numerous collaborative exchanges with us over the years.

Abstract. We report herein dicarbonyl(pentamethylcyclopentadienyl)(ferroceniumyl)iron hexafluorophosphate, which contains a dimetallic cation with a remarkably stable mixed-valent (MV) structure and unexpected redox features. The electronic structure of this compound is discussed in the light of the existing Hush model, which suggests an unusually strong electronic coupling between the two iron centers, despite the non-symmetric environment of the metallic centers. End-to-end charge delocalization is not the main contributor to the extra-large stability of this MV complex, which originates from electronic effects other than the energetic difference between the two MV redox isomers (ΔG^0). This open-shell derivative has also been briefly tested as a catalyst in the reductive etherification of aldehydes by hydrosilanes.

Keywords. Dinuclear Complex; Mixed-Valence Complex; Ferrocene; Carbonyl Complex; Cyclic Voltammetry; Etherification of Aldehydes

1. Introduction

Some years ago, we reported a new family of iron(II) complexes based on the [Fe(η^5-C$_5$Me$_5$)(CO)$_2$] (Fp*) core, some of which were used as precatalysts (Scheme 1; **1a-c**) for the UV-promoted reductive etherification of carbonyl compounds by dialkoxysilanes.[1-2] In recent years related transformations have attracted a sustained interest.[3-7] During these studies,[1] we also reported the ferrocene-containing analogue **2**, in which the redox-active ferrocenyl unit (Fc) was exploited to exert redox-control over this catalytic transformation,[8] a topical concern in catalysis.[9-11] In order to explore this further, we now report the extensive characterization of the mono-oxidized derivative of **2** which is a non-symmetric Fe(II)/Fe(III) MV complex whose behavior can, as we shall see, be analyzed in the light of Hush theory.[12-16] Finally, some preliminary results of its catalytic performance for the aforementioned reductive etherification will be reported.
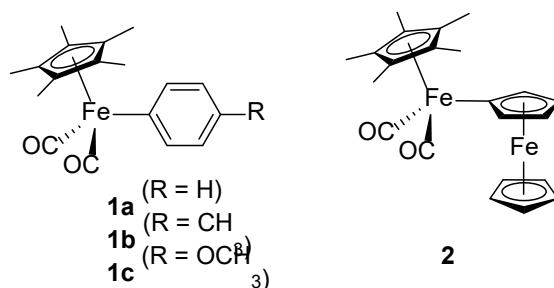
Scheme 1. Organoiron catalysts for the reductive etherification of aldehydes.

2. Experimental

2.1. General Considerations

All manipulations were performed under an atmosphere of argon using standard Schlenk techniques. Solvents were distilled and deoxygenated prior to use. The starting material Cp*Fe(CO)$_2$Fc (**2**) was prepared according to our previous work,[1] while other chemicals were obtained commercially and used without further purification. High-field NMR spectra were obtained on a multinuclear Bruker 300 MHz instrument. Chemical shifts are given in parts per million (ppm) relative to tetramethylsilane

(TMS) for ^{1}H NMR spectra. Transmittance-FTIR spectra were recorded using a Bruker IFS28 spectrometer (400-4000 cm^{-1}). Cyclic voltammograms were recorded using a PAR 263 instrument in methylene chloride at 20 °C (0.1 M [n-Bu$_4$N][PF$_6$]) with 100 mV/s scan rate at a platinum disk (1 mm diameter) using a SCE reference electrode and ferrocene as internal calibrant (0.46 V).[17] Photolyses were performed with a Heraeus UV lamp (TQ150, 150 W, medium pressure) equipped with a quartz jacket. ESR X-Band spectra were recorded on a Bruker EMX-8/2.7 (X-band) spectrometer. Mössbauer spectra were recorded with a 2.5 x 10^{-2} C (9.25 x 10^8 Bq) ^{57}Co source using a symmetric triangular sweep mode in the LCC (Toulouse). The spectrometer calibration was effected using natural iron foil at 20 °C and all isotropic shifts (IS) are reported with respect to the centroid of this spectrum. Mass spectrometry (MS) analyses were performed at the "Centre Regional de Mesures Physiques de l'Ouest" (CRMPO, University of Rennes) on a high-resolution MS/MS ZABSpec TOF Micromass Spectrometer.

2.2. Dicarbonyl(pentamethylcyclopentadienyl)(ferroceniumyl)iron Hexafluorophosphate (2[PF$_6$])

A solution of complex **2** (0.160 g, 0.37 mmol) and ferrocenium hexafluorophosphate (0.116 g, 0.35 mmol) in THF (15 mL) and methylene chloride (10 mL) was stirred for 1 h. After evaporation to dryness, the brown residue was purified by partial precipitation from methylene chloride and diethyl ether, washed with diethyl ether (10 mL) and n-pentane (10 mL), and then dried in vacuo to afford complex **2**[PF$_6$] as a brown powder (0.180 g, 89%). Crystals suitable for a single-crystal X-ray diffraction study were grown by slow diffusion of n-pentane into a saturated methylene chloride solution of complex **2**[PF$_6$]. Mp. 252 °C (dec.). HRMS (ESI/CH$_2$Cl$_2$): [M]$^+$ (C$_{22}$H$_{24}$Fe$_2$O$_2$) requires 432.0469, found 432.0468. IR (CH$_2$Cl$_2$): 2007 (s, $\nu_{C\equiv O}$), 1959 (s, $\nu_{C\equiv O}$), 849 (s, ν_{P-F}). ^{1}H NMR (300 MHz, CD$_2$Cl$_2$): $\delta = 6.1$ (s, 15H), 24.9 (broad s, 5H), 38.8 (broad s, 2H), 49.4 (broad s, 2H). CV (CH$_2$Cl$_2$): $E^0_1 = 0.10$ V ($\Delta E_p = 0.12$ V, $I_p^a/I_p^c = 1.0$); $E^0_2 = 1.38$ V ($\Delta E_p = 0.12$ V, $I_p^a/I_p^c = 0.7$). UV–Vis–near-IR (CH$_2$Cl$_2$): λ_{max} ($\varepsilon/10^3$ M^{-1}.cm^{-1}) 250 (24.9), 278 (sh, 15.7), 340 (sh, 4.2), 420 (3.2), 568 (sh, 0.2), 890 (0.8). ESR (CH$_2$Cl$_2$/1,2-C$_2$H$_4$Cl$_2$, 80 K): $g_{\parallel} = 3.67$, $g_{\perp} = 1.77$.

2.3. Reductive Etherification of p-Bromobenzaldehyde with 2[PF$_6$]

In a Schlenk tube under 1 atm of argon, a solution of *p*-bromobenzaldehyde (2 mmol), **2**[PF$_6$] (0.04 mmol, 23 mg), and diethoxymethylsilane (0.40 g, 3.0 mmol, 370 mg) in CH$_2$Cl$_2$ (15 mL) was irradiated for 4 h. After removal of the solvent, methanol (5 mL) and aqueous NaOH solution (2.5 M, 5 mL) were added and the resulting suspension was stirred overnight. Neutralization with aqueous HCl solution (2 M, 30 mL) and brine (20 mL), followed by extraction of the reaction mixture with diethyl ether, washing of the extract with water and drying over anhydrous magnesium sulfate, filtration and evaporation to dryness, gave 1-bromo-4-(ethoxymethyl)benzene as a pure yellow oil (380 mg, 1.78 mmol; 88%).

2.4. X-ray Diffraction Study

Data collection of **2**[PF$_6$] was carried out on a Bruker Apex-II CCD diffractometer at 150 K. The structure was solved by direct methods using the *SIR97* program,[18] and then refined with full-matrix least-squares methods based on F^2 (*SHELXL-97*) [19] with the aid of the *WINGX*[20] program. All non-hydrogen atoms were refined with anisotropic atomic displacement parameters. H atoms were included in the final cycle of refinement in their calculated positions. Details of the data collection, cell dimensions, and structure refinement are given in Table S1 (Supporting Information). CIF files for **2**[PF$_6$] have been deposited at the Cambridge Crystallographic Data Center and were allocated the deposition number CCDC 863975.

3. Results and Discussion

3.1. Synthesis and Characterization of 2[PF$_6$]

A cyclic voltammetric study of **2** was conducted first, to obtain information about the oxidation of its electron-rich ferrocenyl (Fc) fragment (Supporting Information). Some unexpected features were

immediately seen. The first oxidation occurs at a much lower potential (-0.36 V *vs.* FcH) than that of ferrocene, although the Fp* group was not expected to be very strongly electron-releasing given the electron-withdrawing nature of its two carbonyl ligands (e.g. oxidation potentials much above that of ferrocene are found for complexes **1a-c** [0.48-0.61 V *vs.* FcH]). The second oxidation, presumed to be localized on the Fp* moiety, occurs at a significantly higher potential (+0.92 V *vs.* FcH) than in **1a-c** and exhibits partial chemical reversibility on the timescale of the measurement, whereas **1a-c** are irreversible under similar conditions. This indicates a kinetic increase in the stability of the dication 2^{2+} compared to the cations $1a\text{-}c^{+}$. Furthermore, considering the potential difference between the two redox events ($\Delta E° = 1.28$ V), the monocation 2^{+} appears to be a very stable Fe(II)/Fe(III) mixed-valent (MV) complex on thermodynamic grounds, with a stability constant (K_c) ≈ 4.95 x 10^{21} (eq. 1) for the corresponding comproportionation reaction (eq. 2).

$$K_c = 10^{(\Delta E°/0.059)} \qquad (1)$$

$$2^{+} + 2^{+} \Leftrightarrow 2 + 2^{2+} \qquad (2)$$

We therefore decided to isolate and characterize this open-shell compound following chemical oxidation of **2** using ferrocenium hexafluorophosphate as a chemical oxidant (Scheme 2). The salt **2**[PF$_6$] was isolated as a brown powder and subsequently crystallized, affording access to its structural data in the solid state (Figure 1). In this compound, the ν_{CO} stretching modes are shifted to higher wavenumbers compared to those of **2**, namely 1959 and 2007 cm^{-1} (*vs.* 1935 and 1992 cm^{-1} for **2**), indicating a significant decrease in the retrodonation of the iron(II) to the CO ligands after oxidation of the ferrocenyl unit ($\Delta \bar{\nu}_{CO}$ = +24 and +15 cm^{-1}, respectively).[1] Note that these wave numbers remain lower than those found for the acetonitrile complex [Fe(η^5-C$_5$Me$_5$)(CO)$_2$(NCMe)][PF$_6$] (**3**[PF$_6$]; 2048 and 1996 cm^{-1}) or related Fe(II) cationic derivatives,[21-24] in line with delocalization of comparatively less amount of positive charge. In the IR spectrum of **2**[PF$_6$], an absorption at 879 cm^{-1}, close to the

---

[1]Differences of only +3 cm^{-1} for each $\bar{\nu}_{CO}$ mode are stated between **1a** and **2**.[1]

strong PF_6^- mode, probably corresponds to a δ_{CH} mode of the Cp protons around the ferrocenium center. This vibrational mode, which has often been used as a redox marker for ferrocene/ferrocenium derivatives,[25] is observed at 823 cm^{-1} in **2**. The ^1H NMR spectrum of this paramagnetic MV cation **2**[PF$_6$] in CD_2Cl_2 reveals large down-field shifts for the various Cp protons at 24.9 ppm (unsubstituted Cp) and 38.8/49.4 ppm (substituted Cp), i.e. values bracketing the isotropic shift reported for the corresponding nuclei in [FcH][PF$_6$] (*ca.* 26 ppm in acetone-d^6),[26-27] while the ESR spectrum at 77 K in a CH_2Cl_2/1,2-$C_2H_4Cl_2$ glass reveals an axial signal for the unpaired electron ($g_\parallel = 3.47$; $g_\perp = 1.83$; $\Delta g = 1.64$) similar to that obtained for solid samples of [FcH][I$_3$] at the same temperature ($g_\parallel = 3.67$; $g_\perp = 1.77$; $\Delta g = 1.90$);[26] the lower anisotropy seen for **2**[PF$_6$] is to be expected when one Cp ring is substituted.[27-28] Finally, Mössbauer spectroscopy points to a localized valency for **2**[PF$_6$] (see Supporting Information). Thus, the doublet corresponding to the Fe(II) site of Fc* in **2** remains nearly unchanged in **2**[PF$_6$], while the second doublet of **2** with the largest quadrupolar splitting and which corresponds to the Fe(II) of the Fc site of **2** collapses in a broad signal characteristic of Fe(III) in ferrocenium after chemical oxidation,[29-30] a situation resembling that reported for the extended analogue of **2**$^+$ discussed later on (**4a**[DDQ]; Scheme 3).[31]
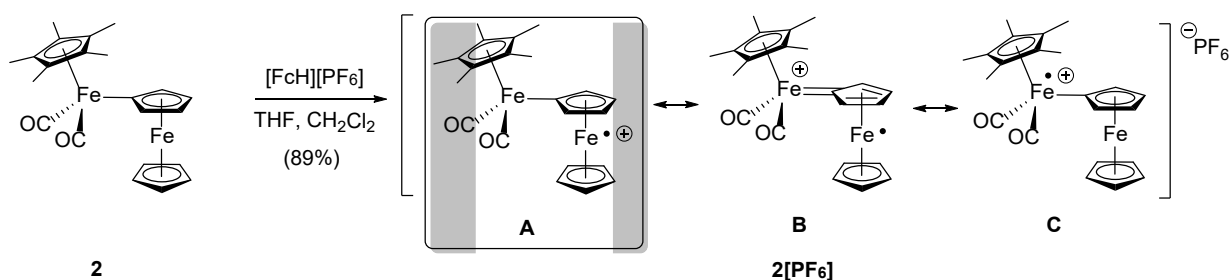
Scheme 2. Synthesis of the MV complex **2**[PF$_6$]. Its dominant VB form is boxed.

The solid-state structure of **2**[PF$_6$] (Figure 1) reveals expansion in the coordination sphere around the ferrocenyl moiety (lengthening of the Fe(2)–Cp$_{centroid}$ bond from 1.653 Å for **2** to 1.715 Å for **2**$^+$), and consistent with a decreased back-donation of the ferrocenyl-based iron center, formally in the Fe(III)

redox state, resulting in a weakening of the Fe-Cp* bond. Furthermore, the elongation of the Fe(1)–C(O) bonds (from 1.752(2)/1.760(2) Å for **2** to 1.766(2) Å for **2$^+$**) and the shortening of the C(11)–O(12) bond (from 1.148(2)/1.152(2) Å for **2** to 1.145(2) Å for **2$^+$**) at the iron carbonyl center, in agreement with the infrared results, suggest a decrease in retrodonation at Fe(1) in **2**[PF$_6$] (which is formally in the Fe(II) redox state). Finally, some delocalization of the electron density from this Fe(II) center to the ferrocenium unit is evidenced by a significant decrease in the mean Fe(1)–C(21) distance from 1.985(2) Å for **2** to 1.964(2) Å for **2$^+$**, in line with some increase in the bonding character of this bond. Thus, resonance of the VB form A (dominant) with a carbene-like mesomer such as B can be deduced from the changes taking place following oxidation of **2** to form **2$^+$**. Considering 1.857(6) Å as the typical Fe-C bond length for a Fp* cationic carbene complex,[32] and the Fe-C bond length of **1a** (2.005(1) Å)[1] as reference for a single metal-aryl bond in Fp*-type neutral complexes, the contribution of mesomer B is estimated to be 29% based on the available metric data for that compound. If **2** is considered as a reference compound instead of **1a**, this percentage drops to 17 %, so that a weight around 20% can be inferred for B relative to A in the ground state (GS) for **2**[PF$_6$].[2]
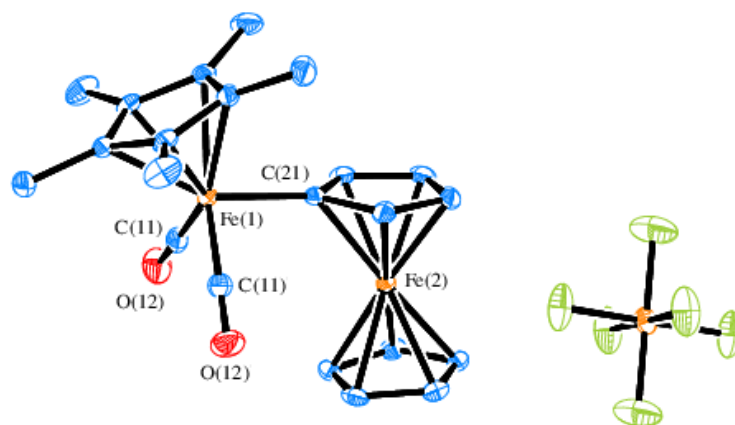

Figure 1. Molecular diagram of the MV complex **2**[PF$_6$] at the 40% probability level. Selected bond lengths (Å) and angles (°): Fe(1)–C(11) 1.766(2), Fe(1)–C(21) 1.964(2), C(11)–O(12) 1.145(2), Fe(1)–

---

[2] As underlined by one referee, this assumes a linear relationship between bond length and bond order which is often not the case. This figure should therefore be taken as a gross estimate (±10 %).

Cp*$_{centroid}$ 1.736, Fe(2)–Cp$_{centroid}$ 1.715 Å, C(11)–Fe(1)–C(11) 96.00(1), C(11)–Fe(1)–C(21) 92.33(8), O(12)–C(11)–Fe(1) 178.60(1), C(21)–Fe(1)–Cp*$_{centroid}$ 119.77, C(11)–Fe(1)–Cp*$_{centroid}$ 124.04°.

3.2. Electronic Structure of 2[PF$_6$]

Evaluating the contribution of the various valence bond (VB) mesomers contributing to the ground state (GS) description of **2**[PF$_6$] is important when ferrocene is used as a redox switch, since this describes how the influence of oxidation is actually transmitted to the catalytic (Fp*) site. While crystallographic data strongly suggest the participation of mesomer B, evidence for the participation of mesomer C (formally the MV isomer of A) is more difficult to obtain. Both B and C would afford the strong increase in carbonyl stretching frequency seen following oxidation of **2**, while ESR and NMR spectroscopies indicate an open-shell structure strongly resembling that of ferrocenium, and thus a dominant contribution of A (or B) relative to C (for which a rhombic ESR signal with a lower anisotropy would be expected). The larger isotropic shifts observed for the protons of the substituted ring are also indicative of some increased spin polarization on that ring,[26] consistent with a resonance contribution from a VB mesomer such as B. Overall, these data along with the Mössbauer data indicate an oxidation localized on the ferrocene part of **2**[PF$_6$] in line with a class-I or -II mixed valence structure in the classification of Robin and Day, suggesting that the weight of C is minor compared to that of A or B.[13, 33] In order to discover more about the participation of the VB form C to the bond description and to establish the class of the MV complex, we decided to look for an intervalence charge-transfer (IVCT) band for this MV complex, so as to evaluate the electronic coupling between A and C based on Hush theory. The electronic-absorption spectra of **2** and **2**[PF$_6$] were thus measured in the UV-visible range (Figure 2a).

A tentative attribution of the absorptions observed for **2** can be proposed because they resemble those observed for **1a-c** (see Supporting Information), but appear twice as intense. This similarity is unsurprising, given that the forbidden ligand-field (LF) absorptions of ferrocene are usually quite weak ($\varepsilon < 50$), with the lowest-energy strong (MLCT) absorption occurring near 265 nm.[34] Thus, the LF

absorptions of the ferrocenyl part of **2** must be masked by more significant absorptions (they possibly give rise to the weak shoulder observed near 440 nm), while the lowest-energy strong MLCT band, slightly blue–shifted by the electron-releasing Fp* substituent, is not observed within the surveyed spectral range (wavelengths greater than 250 nm). Due to its insensitivity to substituent effects in **1a-c**, the less intense transition detected near 380 nm is attributed to the (forbidden) LF transition at the origin of the photo-ejection of one carbonyl ligand (when **2** or **1a-c** are employed as photocatalysts),[1, 23] while that at somewhat higher energy, near 350 nm, probably corresponds to an (allowed) $d_{Fe} \rightarrow \pi^*_{CO}$ (MLCT) transition in view of the modest substituent effect undergone by the corresponding transitions in **1a-c**.

These two bands do not appear to be much affected by oxidation, in proceeding to **2**[PF$_6$], apart from a 15 nm shift to higher energies for the band near 350 nm. In contrast, a new band appears at 420 nm, and another band of lower intensity appears at 888 nm. This is expected since, upon oxidation, the first LF bands are found at lower energies in ferrocenium than in ferrocene. Of the allowed transitions, ligand-to-metal charge transfer (LMCT) transitions in ferrocenium replace the MLCT transitions of ferrocene and appear at lower energies.[34] The lowest energy band for ferrocenium salts corresponds to a $\pi_{Cp} \rightarrow d^*_{Fe}$ LMCT transition, often of low intensity ($\varepsilon < 10$ in ferrocenium), and has been shown to be strongly sensitive to substituents effects, electron-releasing substituents on the cyclopentadienyl ring(s) shifting it to lower energies,[34-35] possibly from mixing some substituent character into the HOMO. For **2**[PF$_6$], the new band that appears at 890 nm (band A, Figure 2b) is unlikely to be a forbidden LF transition, given its intensity (*ca.* 800 M.cm^{-1}). Instead, it likely corresponds to a CT transition of ferricinium,[36] and more specifically an intervalence charge transfer (IVCT), given the large organometallic character of the ring substituent in **2**[PF$_6$].[31, 37] The weak shoulder observed near 568 nm (Band B) possibly corresponds to the lowest-energy LF absorption associated with the ferrocenium moiety, while the second and more intense transition observed near 420 nm (band C) corresponds to the first true $\pi_{Cp} \rightarrow d^*_{Fe}$ (LMCT) band of the ferrocenium unit in **2**[PF$_6$].
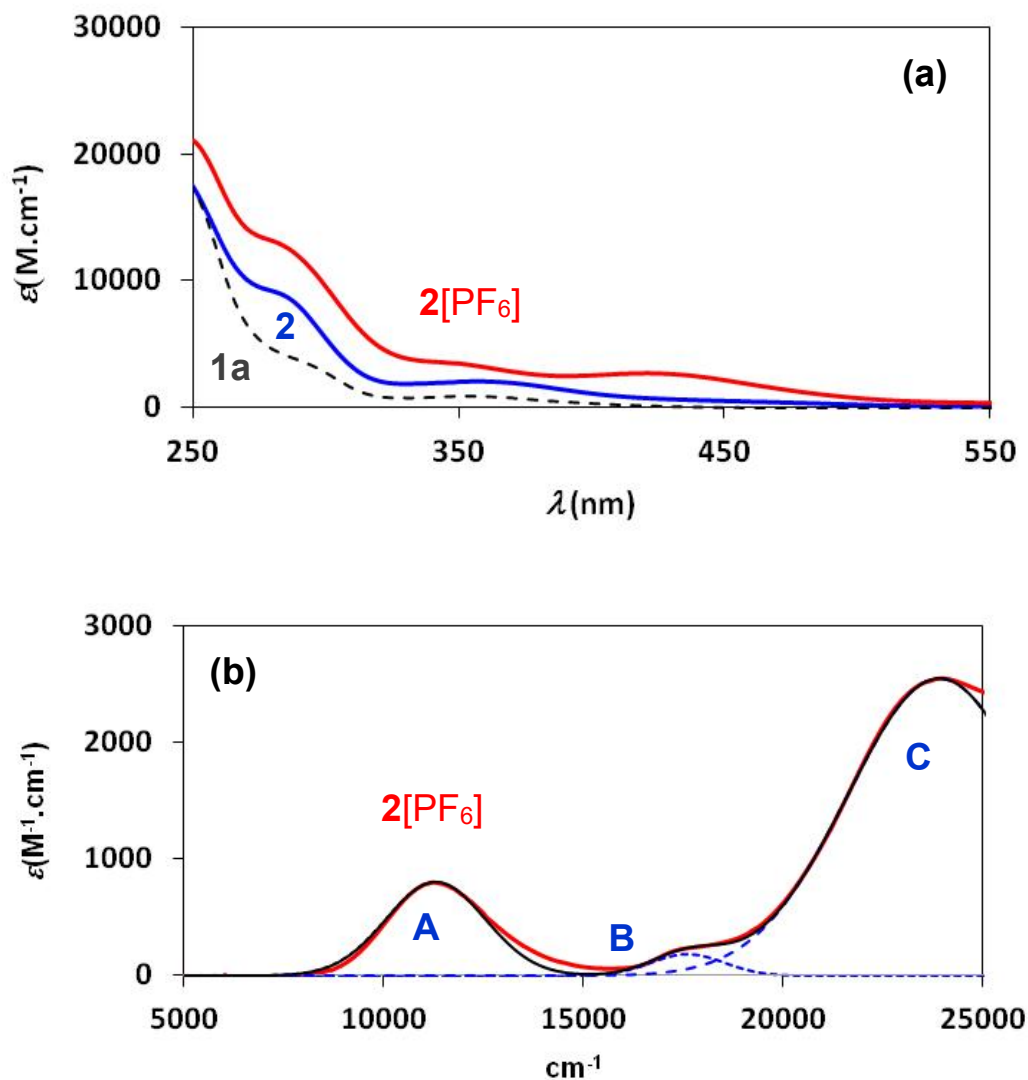
Figure 2. (a) UV-vis spectra of **1a**, **2** and **2**[PF$_6$] in CH$_2$Cl$_2$. (b) Deconvolution of the near-infrared part of the spectrum of **2**[PF$_6$] (sum spectrum in black): band A is the IVCT band, while band C corresponds to the band of **2**[PF$_6$] observed at 425 nm in (a).

Following a classic approach,[37] we have therefore deconvoluted this IVCT band (A) into its Gaussian components (Figure 2b) and used eqs 3-4,[3] based on Hush theory for unsymmetrical class-II

---

[3] In these equations, ε_{max}, $\bar{\upsilon}_{max}$ and $\Delta\bar{\upsilon}_{1/2}$ are the extinction coefficient, the energy of the maximum and the halfwidth of the IVCT band, respectively, while ΔG^0 is the energy difference between the MV isomers (A and B).

MV complexes, to derive the electronic coupling (see Supporting Information section for details).[15, 38] The second band (B) at higher energy was also considered as a potential IVCT transition, but was eventually discarded based on linewidth considerations. As proposed earlier, it therefore more likely corresponds to the lowest energy LF band of the ferrocenium group. In line with our hypothesis, band A undergoes a hypsochromic shift in proceeding to more polar solvents whereas band B appears unaffected by the change in solvent (see Supporting Information).

$$H_{MM'} = (2.06.10^{-2}/d_{MM'})(\varepsilon_{max}\ \bar{\upsilon}_{max}\ \Delta\bar{\upsilon}_{1/2})^{1/2} \tag{3}$$

$$(\Delta\bar{\upsilon}_{1/2})_{theo} = [2310.(\ \bar{\upsilon}_{max} - \Delta G^0)]^{1/2} \tag{4}$$

Several conclusions can be drawn from this analysis. An electronic coupling ($H_{MM'}$) of 880 ± 20 cm^{-1} can be derived, but the bandwidth for this IVCT band is less than that expected based on theory (2914 cm^{-1} found vs. 3970 cm^{-1} predicted from eq. 4). Part of this discrepancy is related to the uncertainties in the estimation of the ΔG^0 term (ca. 4470 cm^{-1}) which has been derived from the difference between the oxidation potentials of FcH and **1a**. While some error results from the determination of the oxidation potential of **1a** (Supporting Information), the largest source of uncertainty originates from the fact that the model used (eqs 3 and 4) does not take into consideration other sources of stabilization of the MV complex (A) distinct from mesomery with its redox isomer (C). Nevertheless, the $H_{MM'}$ found still constitutes a fair approximation of the actual value, and it can be used to afford an estimate of the mixing coefficient (α) between the diabatic states (i.e. mesomers A and C) in the GS (eqs 5-6).[39] The value of α (0.078) reveals that VB mesomer C participates to only a minor extent (< 1%) in the ground state description of **2**[PF$_6$]. We note that this value compares to that reported (0.096) for **4b**$^+$ an homologue of **2**$^+$ featuring an alkynyl spacer between the ferrocenyl and Fp* groups and for which a

lower electronic coupling can be derived ($H_{MM'} \approx 716$ cm^{-1}),[31] in line with the increased distance between the redox sites in **4b$^+$**.[4][16]

$$\alpha^2 = (H_{MM'}/\bar{\upsilon}_{max})^2 \tag{5}$$

$$\Psi_{Ground\ State} = (1-\alpha^2)^{-1/2}[\Psi_A + \alpha\Psi_C] \tag{6}$$

$$e \times \Delta E^0 = \Delta G^0 + \Delta G_E + \Delta G_D + \Delta G_S + \Delta G_{EF} + \Delta G_{IP} + \Delta G_M \tag{7}$$

The increase seen in the difference in first and second oxidation potentials of **2** ($\Delta E^0 = 1.28$ V) compared to that between the redox potentials of the mononuclear model compounds ($\Delta G^0/e = 0.55$ V) reflects the gain in thermodynamic stability by the MV complex **2$^+$** compared to that of the non-interacting parts (in **1a** and ferrocene). This increase is usually attributed to several well-known contributions (eq. 7).[16, 40] From our study (Supporting information), it is clear that the delocalization term (ΔG_D or mesomery between A and C) will not contribute much to the large difference found (0.73 V), while the so-called entropic factor (ΔG_E) is also too weak for making a significant contribution. Among the remaining factors, we believe that the electrostatic force factor (ΔG_{EF}) and synergic factor (ΔG_S) comprise the major contributions. Thus, electrostatic repulsion in **2^{2+}**,[5] which can be estimated to be around 0.45 eV using the expressions for spherical point charges, will favor comproportionation, as will the electronic relaxation of the MV complex exemplified by the mesomery between A and B.[6] This additional stabilization is also at the origin of the low value found for the first oxidation potential of **2**. Indeed, the latter are reminiscent of values reported for several aminoferrocenes (**5a**; Scheme 3) that were also unanticipated based on simple substituent effects (Hammett coefficients).[41] The strong

---

[4] Also, a less pronounced change in the carbonyl stretching modes ot the Fp* part has been reported ($\Delta\bar{\upsilon}_{CO} = +8$ cm^{-1} for **4b/4b$^+$** *vs.* $\Delta\bar{\upsilon}_{CO} = +20$ cm^{-1} for **2/2$^+$**), in line with a lower impact of oxidation on the remote redox site in the former set of compounds.

[5] In line with the importance of the electrostatic force factor on the first redox potential of **2**, we note that the first oxidation potential reported for its longer homologue **4b** takes place at higher potential (-0.1 V vs. FcH).

[6] The importance of the synergic factor for **4b$^+$** (i.e. mesomery with a VB structure resembling B) is reflected by a increase of +16 cm^{-1} of one of the modes relative to **2**.

resemblance of the spectral features in the low-energy region independently reported for the cation [FcN(p-Tol)2][BF4] (**5b**[BF4]) with those observed for **2**$^+$ suggest that similar explanations might be applicable to aminoferrocenes.[36] However, with **2**, the second oxidation takes place at higher potentials, resulting in a thermodynamically (and possibly kinetically)[7] more stable monocation than most aminoferrocenyl-derived monocations reported so far and also than its Fp analogue **6**$^+$,[42] pointing at the importance of the Cp permethylation in **2**$^+$.
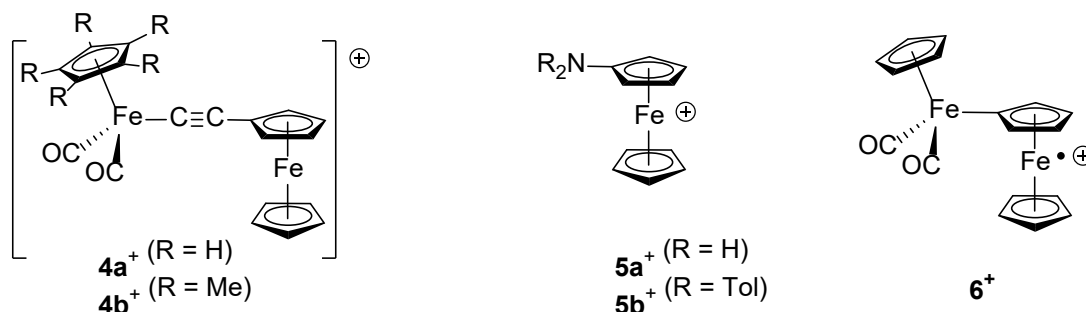

Scheme 3. Selected ferrocenium derivatives related to **2**$^+$.

3.3. Catalysis

Finally, we also briefly investigated the catalytic activity of **2**[PF6] in the reductive etherification of aldehydes. This reaction was performed using 4-bromobenzaldehyde as the model substrate, under the conditions previously optimized (Scheme 4).[1] Interestingly, the same yield of 1-bromotolyl-4-(ethoxymethyl)benzene was obtained as when its reduced parent **2** was used as catalyst, in spite of the fact that the Fp* center is now significantly more electron deficient, cationic, and possesses some radical character. While this result suggests that the rate of the transformation is not significantly modified by oxidation of the precatalyst over a standard run, alternative explanations could also be that (i) either the precatalyst is rapidly reduced back under the reaction conditions before the catalysis starts or that (ii) the organometallic (Fc) σ-ligand initially present on the precatalyst is lost during formation

---

[7] Based on the reported chemical reversibility of the CVs. As a matter of fact a sample of **2**[PF6] was kept over three year in a opaque glass vial at 20 °C in air without apparent decomposition.

14

of the active species, a conclusion that would contradict the hypothesis that a decarbonylated 16-e species such as [Cp*Fe(CO)(Fc$^+$)] lies on the catalytic cycle. Regardless if any of these explanations are relevant, this establishes that redox control of this reaction will not be possible with **2** under the conditions previously defined. A better understanding of how oxidation of the precatalyst impacts this transformation and whether redox control can eventually be implemented will require additional work.
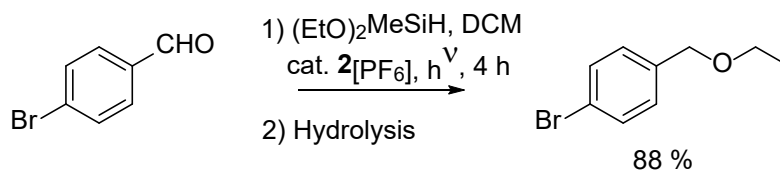
Scheme 4. Catalytic behavior of the iron complex **2**[PF$_6$].

4. Conclusion

In conclusion, we have characterized the cationic oxidation product of the known Fp*-Fc dinuclear complex **2** previously employed as a precatalyst for the photoinduced reductive etherification of aldehydes with functional silanes. We have shown that **2**[PF$_6$] is a non-symmetrical MV complex which belongs to Class IIA in the modified classification of Robin & Day, in spite of the fairly large electronic coupling operative between its two redox centers. Clearly, in addition to the electronic delocalization, several other electronic effects such as charge repulsion in the corresponding dication **2**$^{2+}$ and mesomery contribute to its remarkable thermodynamic stabilization toward disproportionation and explain the fairly low value of its first oxidation potential relative to ferrocene. As such, **2**[PF$_6$] appears as an organometallic "analogue" of several aminoferrocenium derivatives. Furthermore, using the carbonyl ligands as probes, we have shown that oxidation induces a much larger electronic perturbation at the Fp* center than when the Fc group of **2** is replaced by a functional aryl group, as explored previously with the **1a-c** series. In spite of these remarkable properties, we have shown that the use of **2**[PF$_6$] as catalyst for reductive etherification produces comparable yields of the ether product to those of its reduced parent **2** and that redox switching of this reaction is not possible with such a catalyst under the standard conditions previously defined.

Acknowledgements

Appendix A; Supporting Information

Supplementary data associated with this article can be found, in the online version, at http://dx.doi.org/

## References

[1] G. Argouarch, G. Grelaud, T. Roisnel, M.G. Humphrey, F. Paul, Tetrahedron Lett. 53 (2012) 5015-5018.

[2] G. Grelaud, T. Roisnel, V. Dorcet, M.G. Humphrey, F. Paul, G. Argouarch, J. Organomet. Chem. 741-742 (2013) 47-58.

[3] M.L. Tulchinsky, J.R. Briggs, ACS Sustainable Chem. Eng. 4 (2016) 4089-4093.

[4] N. Kalutharage, C.S. Yi, Org. Lett. 17 (2015) 1778-1781.

[5] S.J. Gharpure, J.V.K. Prasad, Eur. J. Org. Chem. (2013) 2076-2079.

[6] B.A. Gellert, N. Kahlcke, M. Feurer, S. Roth, Chem. Eur. J. 17 (2011) 12203-12209.

[7] J.S. Yadav, B.V. Subba Reddy, K. Shiva Shankar, T. Swamy, Tetrahedron Lett. (2010) 46-48.

[8] A.M. Allgeier, C.A. Mirkin, Angew. Chem., Int. Ed. Engl. 37 (1998) 895-908.

[9] O.R. Luca, R.H. Crabtree, Chem. Soc. Rev. 42 (2013) 1440-1459.

[10] F.A. Leibfarth, K.M. Mattson, B.P. Fors, H.A. Collins, C.J. Hawker, Angew. Chem. Int. Ed. 52 (2013) 199-210.

[11] L. Hettmanczyk, L. Suntrup, S. Klenk, C. Hoyer, B. Sarkar, Chem. Eur. J. 23 (2017) 576-585.

[12] A. Ceccon, S. Santi, L. Orian, A. Bisello, Coord. Chem. Rev. 248 (2004) 683-724.

[13] B.S. Brunschwig, C. Creutz, N. Sutin, Chem. Soc. Rev. 31 (2002) 168-184.

[14] K.D. Demadis, C.M. Hartshorn, T.J. Meyer, Chem. Rev. 101 (2001) 2655-2685.

[15] R.J. Crutchley, Adv. Inorg. Chem. 41 (1994) 273-325.

[16] D. Astruc, Electron Transfer and Radical Processes in Transition-Metal Chemistry, VCH Publishers, Inc., New York, 1995.

[17] N.G. Connelly, W.E. Geiger, Chem. Rev. 96 (1996) 877-910.

[18] A. Altomare, M.C. Burla, M. Camalli, G. Cascarano, C. Giacovazzo, A. Guagliardi, A.G.G. Moliterni, G. Polidori, R. Spagna, J. Applied Crystallogr. 32 (1999) 115-119.

[19] G.M. Sheldrick, Acta Crystallogr. A 64 (2008) 112-122.

[20] L.J. Farrugia, J. Appl. Crystallogr. 32 (1999) 837-838.

[21] F. Paul, unpublished results.

[22] L. Bonniard, S. Kahlal, A.K. Diallo, C. Ornelas, T. Roisnel, G. Manca, J. Rodrigues, J. Ruiz, D. Astruc, J.Y. Saillard, Inorg. Chem. 50 (2011) 114-124.

[23] D. Catheline, D. Astruc, Organometallics 3 (1984) 1094-1100.

[24] D. Catheline, D. Astruc, J. Organomet. Chem. 226 (1982) C52-C54.

[25] J.A. Kramer, D.N. Hendrickson, Inorg. Chem. 19 (1980) 3330-3337.

[26] S.E. Anderson, R. Rai, Chem. Phys. 2 (1973) 216-225.

[27] R.B. Materikova, V.N. Babin, S.P. Solodovnikov, I.R. Lyatifov, P.V. Petrovsky, E.I. Fedin, Z. Natuforsch 35b (1980) 1415-1419.

[28] R. Prins, Mol. Phys. 19 (1970) 603-620.

[29] G.K. Wertheim, R.H. Herber, J. Chem. Phys. 38 (1963) 2106-2111.

[30] R.J. Webb, M.D. Lowery, Y. Shiomi, M. Sorai, R.J. Wittebort, D.N. Hendrickson, Inorg. Chem. 31 (1992) 5211-5219.

[31] M. Sato, Y. Hayashi, N. Shintate, M. Katada, S. Kawata, J. Organomet. Chem. 471 (1994) 179-184.

[32] G. Poignant, S. Nlate, V. Guerchais, A.J. Edwards, P.R. Raithby, Organometallics 16 (1997) 124-132.

[33] M.B. Robin, P. Day, Adv. Inorg. Chem. Radiochem. (1967) 247-422.

[34] Y.S. Sohn, D.N. Hendrickson, H.B. Gray, J. Am. Chem. Soc. 93 (1971) 3603-3612.

[35] R. Prins, J. Chem. Soc. D: Chem. Commun. (1970) 280-281.

[36] A. Mendiratta, S. Barlow, M.W. Day, S.R. Marder, Organometallics 18 (1999) 454-456.

[37] N. Gauthier, C. Olivier, S. Rigaut, D. Touchard, T. Roisnel, M.G. Humphrey, F. Paul, Organometallics 27 (2008) 1063-1072.

[38] C. Creutz, Prog. Inorg. Chem. 30 (1983) 1-73.

[39] F. Paul, C. Lapinte, Coord. Chem. Rev. 178/180 (1998) 431-509.

[40] C.E.B. Evans, M.L. Naklicki, A.L. Rezvani, C.A. White, V.V. Kondratiev, R.J. Crutchley, J. Am. Chem. Soc. 120 (1998) 13096-13103.

[41] W.E. Britton, R. Kashyap, M. El-Hashash, M. El-Kady, M. Herberhold, Organometallics 5 (1986) 1029-1031.

[42] K.H. Pannel, M.G. Gonzalez, H. Leano, R. Iglesias, Inorg. Chem. 17 (1978) 1093-1095.

Graphical Abstract.
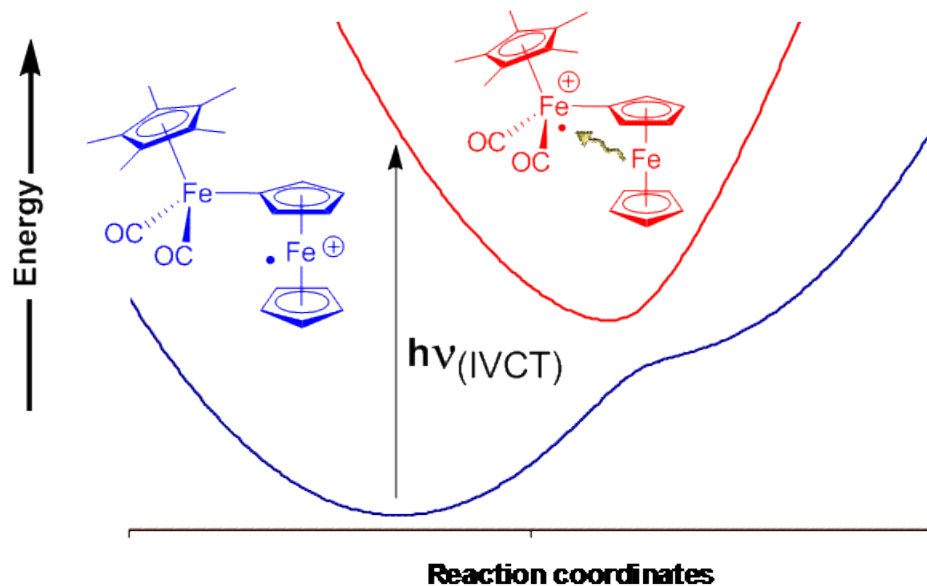
This dimetallic cation possesses a mixed-valent (MV) structure with a very low first redox potential. End-to-end charge delocalization is not the main contributor to its large extra-stability, which instead originates from other electronic effects. This compound can be used as a photocatalyst for the etherification of benzaldehydes by alkoxyalkylsilanes.